Blur on the retina due to higher-order aberrations: Comparison of eye growth models to experimental data

Jennifer J. Hunter
Center for Visual Science, University of Rochester, Rochester, NY, USA

Melanie C. W. Campbell
Department of Physics and Astronomy and School of Optometry, University of Waterloo, Waterloo, ON, Canada, & Guelph Waterloo Physics Institute, Waterloo, ON, Canada

Marsha L. Kisilak
Department of Physics and Astronomy and School of Optometry, University of Waterloo, Waterloo, ON, Canada

Elizabeth L. Irving
School of Optometry, University of Waterloo, Waterloo, ON, Canada

In the simplest model of eye growth, the ocular optics uniformly scale upwards, as do monochromatic higher-order aberrations (HOA) and linear blur on the retina. However, measured HOA remain constant or decrease with growth in some species. A new model, which holds HOA and the associated linear blur on the retina constant, was used to predict changes in HOA and resulting image quality on the retina during growth, in each of chick, monkey, and human. Models used rates of growth in each of the three species. Angular optical quality on the retina due to HOA, and its metrics improved, in contrast to the constancy predicted by uniform scaling. The model with constant linear HOA blur predicts well the improvement in human optical quality between infant and adult. Overall, in chick and monkey, angular blur improves at a rate faster than that predicted by the constant linear blur model, implying that linear retinal blur due to HOA decreases with age. On the other hand, in chick, angular blur due to third-order aberrations decreased at a rate predicted by the constant linear blur model. Growth changes in retinal blur due to HOA are species dependent but can be better understood by comparison with the new model predictions.

Keywords: visual development, physiological optics, emmetropization

Citation: Hunter, J. J., Campbell, M. C. W., Kisilak, M. L., & Irving, E. L. (2009). Blur on the retina due to higher-order aberrations: Comparison of eye growth models to experimental data. *Journal of Vision, 9*(6):12, 1–20, http://journalofvision.org/9/6/12/, doi:10.1167/9.6.12.

Introduction

Eye models describe the optical properties that determine retinal image quality, predict growth-related changes, and give improved understanding of developmental processes. With growth, the optics of the eye change, potentially producing changes in image quality on the retina. Changes in eye length and concurrent changes in the refractive power of the optics produce decreasing refractive error with normal growth (Hirsch & Weymouth, 1990). It is a vision-dependent process, referred to as emmetropization, and occurs in many different species including chicks, monkeys, and humans (Wallman & Winawer, 2004). Young chicks, commonly used as a model of emmetropization, exhibit a decrease in mean ocular refraction (MOR; Irving, Callender, & Sivak, 1991; Schaeffel, Glasser, & Howland, 1988; Wallman, 1991; Wallman, Turkel, & Trachtman, 1978), MOR variability (Irving et al., 1991), astigmatism (Kisilak, Hunter, Huang, Campbell, & Irving, 2008; Schaeffel, Hagel, Eikermann, & Collett, 1994; Schmid & Wildsoet, 1997; Tian & Wildsoet, 2006), and astigmatic variability (Kisilak, Hunter et al., 2008). In monkeys (Qiao-Grider, Hung, Kee, Ramamirtham, & Smith, 2007) and humans (Hirsch & Weymouth, 1990), MOR, as well as astigmatism, and their variability also decrease longitudinally beginning in infancy. In humans, longitudinal chromatic aberration decreases with age from infant to adult, which, combined with increasing pupil size, produces a more constant optical blur (Wang, Candy, Teel & Jacobs, 2008).

In addition to MOR, astigmatism, and chromatic aberration, higher-order monochromatic aberrations (HOA) also contribute to the optical blur (image quality) on the retina (Wetherell, 1980). The impact of HOA on retinal image quality can be quantified by their root mean square (RMS)

doi: 10.1167/9.6.12 Received January 3, 2009; published June 24, 2009 ISSN 1534-7362

across the normalized pupil (HO RMSA). The impact of HOA and diffraction can be analyzed exactly on the retina in real (PSF − point spread function) and frequency (OTF − optical transfer function) spaces or estimated using a geometrical approximation of retinal blur, equivalent blur (EB; Kisilak, Campbell, Hunter, Irving, & Huang, 2006). EB, which ignores diffraction, is simpler to calculate as a function of age than the exact PSF and is a valid metric from which to approximate the age variation of angular blur on the retina (Appendix E).

Schematic eye models have been used to predict optical properties as a function of age for chicks (Irving, Sivak, Curry, & Callender, 1996; Schaeffel & Howland, 1988), and for monkey and human infants and adults (Lotmar, 1976; Qiao-Grider et al., 2007; Rabbetts, 1998). However, they are relatively complicated and predict only paraxial properties, not HOA and retinal image quality. In the simplest models of eye growth, the optics of the eye uniformly expand (Brown, Koretz, & Bron, 1999; Koretz, Rogot, & Kaufman, 1995). If the wavefront error is known at one age, these models can in turn predict changes in retinal image quality, with constant pupils (Howland, 2005; Kisilak, Hunter, Campbell, Irving, & Huang, 2005), or with growing pupils (Kisilak et al., 2005; Wang & Candy, 2005).

Across increasing age, for pupils held constant between 1.5 and 2 mm in chicks (Garcia de la Cera, Rodriguez, & Marcos, 2006; Kisilak et al., 2006; Tian & Wildsoet, 2006) and for 5-mm pupils in monkeys (Ramamirtham et al., 2006), HO RMSA decreased with age. Chick (Garcia de la Cera et al., 2006) and monkey (Ramamirtham et al., 2006) modulation transfer functions (MTFs) also improved as did the monkey PSF (Williams & Boothe, 1981).

Across growing pupils with a nearly constant numerical aperture, HO RMSA in chicks remained almost constant (Kisilak et al., 2006) or decreased slightly (Thibos, Cheng, Phillips, & Collins, 2002). EB exponentially decreased (Kisilak et al., 2006). Similarly, in humans, PSF blur from HOA decreased although HO RMSA did not change significantly between human infants and their parents (Wang & Candy, 2005). In contrast, in monkeys, initially large HOA in infancy decreased rapidly for growing pupils scaled with a constant numerical aperture and the MTF due to HOA improved (Ramamirtham et al., 2006). These age changes with growing pupils are not predicted by current eye models. However, it is known that ocular changes are more complex than uniformly scaled growth (Qiao-Grider et al., 2007; Spooner, 1959; Zadnik, Mutti, Fusaro, & Adams, 1995).

As the role of HOA in emmetropization and refractive error development is not yet understood, it is important to model their longitudinal behavior. In humans, some have found an association between higher amounts of HO RMSA and myopia (Collins, Wildsoet, & Atchison, 1995; He et al., 2002; Llorente, Barbero, Cano, Dorronsoro, & Marcos, 2004; Marcos, Moreno-Barriuso, Llorente, Navarro, & Barber, 2000; Paquin, Hamam, & Simonet, 2002) while others find no association (Carkeet, Luo, Tong, Saw, & Tan, 2002; Porter, Guirao, Cox, & Williams, 2001) or suggest that blur from aberrations is not causal in refractive error development (Carkeet et al., 2002; Charman, 2005). Cross-sectional analyses in humans (Artal, Benito, & Tabernero, 2006; Kelly, Mihashi, & Howland, 2004; Llorente et al., 2004) also come to differing conclusions as to whether HOA changes during emmetropization and possibly refractive error development are primary or secondary. HOA could provide a signal to emmetropization (Campbell, Priest, & Hunter, 2001; Hunter, Campbell, Kisilak, & Irving, 2003; Wallman & Winawer, 2004; Wilson, Decker, & Roorda, 2002) as could chromatic aberration (Rucker & Wallman, 2008) or astigmatism (Hunter et al., 2003; Kee, Hung, Qiao, Habib, Smith, 2002; Kisilak, Hunter et al., 2008).

Kisilak et al. (2006) hypothesized that the observed decrease in monochromatic EB (due to HO RMSA) in chicks with growing pupils may be a component of emmetropization. Tian and Wildsoet (2006) hypothesized that HO RMSA emmetropized. HOA in a number of species are affected by visual experience (Kisilak et al., 2006; Kröger, Campbell, & Fernald, 2001; Ramamirtham et al., 2006). However, Ramamirtham and co-authors have suggested that decreases in HOA (Ramamirtham et al., 2006) with growth in normally developing monkeys with increasing pupils and changes observed with lens induction of myopia (Ramamirtham et al., 2007) are secondary to emmetropization of refractive error.

Models of eye growth could help resolve the debate over the primary or secondary nature of the observed changes in HOA. Furthermore, there is a need for additional models of eye growth that would simplify potentially complex changes in the optical components into changes in the wavefront aberrations and predict aging changes in image quality. The new model, described here, has constant linear blur on the retina and constant HO RMSA with growth. It is motivated by the measurement of near constant HO RMSA in chicks and humans. Model validation requires corresponding image quality measurements with increasing pupil size. These are currently available for chicks (Kisilak et al., 2006), monkeys (Ramamirtham et al., 2006), and humans (Wang & Candy, 2005). Thus we will compare predictions from wavefront models with experimental measurements for these three species.

Methods

In three species, we compare two wavefront model predictions with measured age-dependent changes in optical quality. Using age-dependent scaling, based on empirical data (Irving et al., 1996; Qiao-Grider et al., 2007; Wang & Candy, 2005), we calculate the changes in the optical quality of chick, monkey, and human eyes predicted by each model. In chicks, we also calculate image quality predictions from schematic eye models. These predictions are compared to aberration data (Kisilak et al., 2006; Ramamirtham et al., 2006; Wang & Candy,

2005) and to corresponding calculated changes in the optical image on the retina.

Metrics of image quality are single values that describe some property of the image (Appendix A). Changes in metrics as a function of age, predicted by the models, are compared to those measured experimentally or calculated from experimental changes in HOA. Metrics used included those relative to the diffraction limit, such as HO RMSA and Strehl ratio, as well as absolute image quality metrics such as EB, PSF area at half-height, PSF equivalent width, area under the radially averaged MTF, and MTF entropy (Appendix A).

Description of optical models of eye growth

We consider two wavefront models of eye growth for chick, monkey, and human and a schematic eye for chick. The first model is of uniformly scaled growth (Movie 1), analogous to previous models for chick (Kisilak et al., 2005) and human (Wang & Candy, 2005). All ocular dimensions increase proportionally with age (Hunter, Kisilak, Campbell, Irving, & Huang, 2006; Kisilak et al., 2005; Wang & Candy, 2005), thereby keeping the *f*-number constant. The second model with constant linear retinal blur is novel (Movie 2). Constant HO RMSA combined with a paraxial scaling that maintains a constant *f*-number with growth will be shown to give constant linear blur on the retina.

For each species, the predicted changes in HO RMSA and image quality for uniformly scaled and constant linear blur eye models can be calculated from the observed scaling, m, of the eye as a function of age. The models' predictions of changes are, in turn, a function of the ocular scaling, m, for a particular species. The models' predictions depend on their optical properties as outlined below.

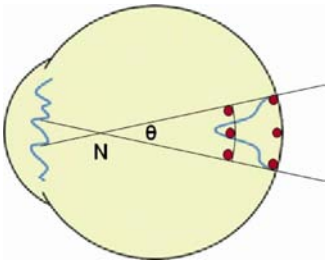

Movie 1. A schematic video representation of uniformly scaled eye growth. With age, all ocular dimensions scale upwards by the same amount. The result is magnified wavefront aberration and linear retinal blur due to HOA. The angular projection of the geometric PSF into object space, θ, remains constant. If the retina also scales upwards, the PSF covers a constant number of cones and angular resolution is constant. HO RMSA increases with age, while equivalent blur (EB) remains constant.

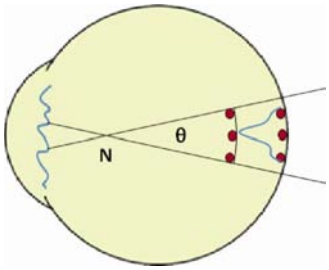

Movie 2. A schematic video representation of eye growth with constant linear retinal blur. With age, all ocular dimensions and paraxial optics scale upwards, but the optics alter such that the linear blur on the retina due to HO RMSA remains constant. This corresponds to a constant wavefront aberration, which is stretched in the increasing pupil. The angular projection of the PSF into object space, θ, reduces with age to θ'. If the optic pole region of the retina remains unchanged, as shown, the PSF covers a constant number of cones and angular resolution improves. HO RMSA remains constant with age, while equivalent blur (EB) decreases.

Optical properties with uniformly scaled eye growth

In the uniformly scaled model of eye growth, as described previously (Howland, 2005; Kisilak et al., 2005; Wang & Candy, 2005), all ocular components (including the pupil) scale by a factor of m, which varies with age (Movie 1, Appendix B). The constant *f*-number with growth was justified by the small change in *f*-number between infant and adult humans (Wang & Candy, 2005). As a result of scaling, relative image quality metrics get worse with age. For example, the RMSA in chick and monkey increases in proportion to the exponential scaling factor (Table 1). The angular geometrical blur due to HOA and its absolute metric, EB, remain constant (Table 2). The decrease in angular blur due to diffraction gives a slight decrease in overall angular blur with increasing pupil size and age. This is reflected in the slight improvement in the absolute metrics, PSF area at half-height, and MTF entropy (Table 3, Appendix B). Linear retinal blur will increase (Table 4, Appendix B). The model can also be used to predict retinal changes with growth. If retinal sampling stretched proportionally to eye size (Movie 1), then angular resolution of the retina would remain constant with age, but linear resolution on the retina would worsen (Kisilak, Bunghardt, Ball, Irving, & Campbell, 2008). However, the primary focus in this paper is the optical change.

Optical properties of constant linear blur model

In both chicks and humans, it appears that changes, more complex than uniformly scaled growth, result in almost constant HO RMSA with age (Kisilak et al., 2006; Wang & Candy, 2005). In our model with constant linear retinal blur, the eye again increases in size (by a scaling factor, m) maintaining a constant *f*-number, but now the

Species	Uniformly scaled model	Constant linear blur model	Observed
Chick	Increasing; t50 = 46 days	Constant	Decreasing; t50 = 47.5 days*
Monkey	Increasing; t50 = 196 days	Constant	Decreasing; t50 = 18–41 days
Human adult/infant	Increasing; 1.5	Constant (=1)	Increasing; 1.15*

Table 1. Changes in the wavefront error (HO RMSA), a relative image quality metric, with growth. Observed values in this table and Tables 2–4 for chick, monkey, and human are based on previously published results (Kisilak et al., 2006; Ramamirtham et al., 2006; Wang & Candy, 2005) and on new analysis of changes with increasing age. A smaller t50 indicates a faster improvement in image quality with increasing age. For comparisons between adult and infant, a number greater than 1 indicates a decrease in image quality with increasing age. *Not significantly different from a constant value with age.

axial length and optics change so as to maintain a constant linear blur due to defocus and HOA (Table 4), respectively (Movie 2). The dependencies of aberrations, retinal blur, and metrics of retinal image quality on the scaling factor are derived in Appendix C. The constant HO RMSA (Table 1) results in decreasing angular blur (Table 2), proportional with the scaling factor, but constant linear retinal blur. Other relative image quality metrics are also constant. Angular metrics of absolute image quality (Table 3) show an improvement with scaling. The specific mechanics of optical changes are irrelevant; it is the net result on the wavefront aberration that is important. The optics (including cornea, pupil, and crystalline lens) could still change such that their paraxial properties scale, but their peripheral structure and/or alignment could change to keep linear retinal blur and HO RMSA constant, via mechanisms that will be addressed in the discussion. In turn, angular retinal sampling could improve (see discussion of mechanisms).

Determination of rates of eye development: Scaling of ocular parameters for eye models

We determine the proportional change in eye size, m, as a function of age and assess the assumption of constant f-number in our models.

Chick

In chick, for which we have the most complete data set, we fit exponential curves to previously published ocular parameter changes with age (White Rock: Irving et al., 1996; Ross Ross: Kisilak et al., 2006) and to unpublished experimental data from our laboratory for changes in pupil size. This allowed us to determine m and to assess the accuracy of the assumption of the models of constant f-number. The exponential nature of these best fits to chick biometric data and ocular scaling with age led to an m that changed continually and exponentially with age. The time to a 50% increase in eye size from the initial value, t50, was calculated. An envelope of scaling factors (m) with age was determined from the exponentially fit coefficients within which all measured ocular parameters fell.

Monkey

In monkey, we used published values of the changes in ocular biometric parameters (Qiao-Grider et al., 2007; Ramamirtham et al., 2006). In particular, we used t50 values; the time for an ocular dimension (fitted to exponentials that increased or decreased to constant values) to change by 50% of the difference between its initial and final values. Complete data for pupil size changes with age were not available. Therefore, as was done to calculate aberrations as a function of eye size (Ramamirtham et al., 2006), uniformly expanding and constant linear blur models were constructed with pupils and eye sizes that expanded at the same rate (m) as ocular length.

Human

In human, we used published values of ocular scaling from the infant to the adult eye (Qiao-Grider et al., 2007; Wang & Candy, 2005).

Eye model predictions

Schematic eye models of the developing chick

We examined predictions from previously developed, anatomically based schematic chick eye models for days 0,

Species	Uniformly scaled model	Constant linear blur model	Observed
Chick	Constant	Decreasing; t50 = 46 days	Decreasing; t50 = 22 days
Monkey	Constant	Decreasing; t50 = 196 days	Decreasing; t50 = 18–50 days
Human adult/infant	Constant (=1)	Decreasing; 0.67	Decreasing; 0.77†

Table 2. Changes in equivalent blur (EB) due to HOA, an absolute image quality metric, with growth. A smaller t50 indicates a faster decrease in angular blur with increasing age. For comparisons between adult and infant, a number less than 1 indicates an improvement in image quality with increasing age. †Significantly different from 1 but not from 0.67.

Species: Measurement	Uniformly scaled model	Constant linear blur model	Observed
Chick: PSF area at HH	Small improvement	Faster improvement; t50 = 23 days	Fastest improvement; t50 = 7.5 days
Chick: MTF entropy	Small improvement	Faster improvement; t50 = 23 days	Fastest improvement; t50 = 12.3 days
Monkey: Adult/infant area under radial MTF	Small improvement	Larger improvement; 1.44	Largest improvement; 1.6
Human: Adult/infant equivalent width of PSF	Small improvement	Largest improvement; 0.67	Larger improvement; 0.76†

Table 3. Improvements in metrics of angular PSF and MTF due to HOA, measures of absolute image quality, with growth. Among the models and observations, for a given metric and species, a smaller t50 indicates a faster improvement in image quality with increasing age. For comparisons between adult and infant, a number greater than 1 for the MTF area indicates an improvement in image quality, whereas a number less than 1 indicates an improvement in image quality for the PSF width. Improvements are compared among the models and observations (across a row). A uniformly expanding model predicts a small improvement in image quality with age (not quantified) due to the decreased influence of diffraction at larger pupils. †Significantly different from 1 but not from 0.67.

7, 14 (Irving et al., 1996), and 30 (Schaeffel & Howland, 1988). These simplified, rotationally symmetric models approximate the refracting surfaces as spheres and do not consider the gradient of refractive index (GRIN) in the crystalline lens. With age, the pupil radius was increased according to the experimental rate of change (Kisilak et al., 2006). The *f*-number in this model decreases with growth by less than 20%. Axial lengths were adjusted to minimize the Zernike spherical defocus term. Because these models do not incorporate tilts and decentrations of the optical elements, they will predict null asymmetric aberrations. Hence, only the spherical aberration Zernike coefficients (SA) were determined for each model in Code V, normalized to the day 0 value, plotted versus chick age and fit with exponentials.

Ocular scaling of wavefront models

By substituting the determined scaling values (m) at each age into the uniformly scaled and constant linear blur models, predictions of changes in image quality measurements were determined for each of the three species.

Retinal image quality observed in the developing eye

We used previously published HO RMSA and more complete HOA data for 0- to 14-day-old chicks (Kisilak et al., 2006), published HO RMSA and MTF data for monkey eyes as a function of age (Ramamirtham et al., 2006), and published HO RMSA and PSF data for infant and adult humans (Wang & Candy, 2005).

For all three species, from the HO RMSA data, measured at increasing pupil radii, EB was calculated to estimate the angular blur on the retina as a function of age (Appendix D). Linear retinal blur was then calculated from EB (Appendix D).

Chick

For chicks, data were available to separately assess the third- and fourth-order RMSA. The experimental rate of change of EB was found both from individual RMSA and pupil data points and from fits to these data. The chick EBs across age for third- and fourth-order and total HOA were fit with exponentials.

In addition, the Zernike coefficients were recalculated (Schwiegerling, 2002) for each eye on each day for the largest common pupil among that day's images. For each bird, the resulting HOA Zernike coefficients were averaged across frames on each day. The corresponding angular PSFs and OTFs were calculated for HOA (third- and fourth-order) alone and in combination with astigmatism and defocus terms (second-order and up).

Image quality metrics for the PSFs and MTFs were averaged and standard errors were calculated across birds

Species	Uniformly scaled model	Constant linear blur model	Observed
Chick	Increasing; t50 = 46 days	Constant	Decreasing; t50 = 42 days
Monkey	Increasing; t50 = 196 days	Constant	Decreasing; t50 = 18–41 days
Human adult/infant	1.5	Constant (= 1)	1.15*

Table 4. Changes in linear retinal blur (LRB), a geometrical approximation of the change in the linear half-width of the PSF due to HOA with growth. This is an absolute measure of image quality on the retina. A decreasing half-width indicates an improvement in image quality. A smaller t50 indicates a more rapid change (either increasing or decreasing) with increasing age. For comparisons between adult and infant, a number greater than 1 indicates an increase in linear blur on the retina with increasing age. *Not significantly different from a constant value with age.

on each day (Hunter, 2006). These angular metrics were fit with exponential functions of age and their t50s were calculated.

Monkey

Literature values of HO RMSA were calculated for pupil sizes, which changed at the rate of change of eye length (Ramamirtham et al., 2006). HO RMSA appears to decrease exponentially to an almost constant value beyond day 200 while pupil size increases to a maximum. MTF data at a constant *f*-number was also used.

Human

In humans, the change from infant to adult in HO RMSA and PSF were taken from Wang and Candy (2005).

Comparison of predicted and observed retinal image quality

The predictions of change in image quality for each of the two models were compared with the change in image quality given by experimental measurements for each of the three species. In particular, the time courses of HO RMSA, EB, and changes in metrics of PSF and MTF were compared with the two models predictions of their time courses. In chick, differences between prediction and experiment were deemed significant if the t50s ± standard error for the exponential regressions to the experimental data did not overlap with those for the model prediction envelopes. The rate of change of the SA of the schematic eye models for chicks was compared to the SA of the scaled models and to its experimentally observed change.

Results

Optical properties of the eye models

Predictions of the models of eye growth are given in Appendices B and C and illustrated in Movies 1 and 2 for a general scaling of the eye, *m*. Following the determination of *m* for each species, numerical results for chick, monkey, and human eyes are summarized in Tables 1–4.

Wavefront models

Across species

For all models, HO RMSA and the geometric linear blur on the retina are predicted to behave in the same manner, increasing exponentially in the expanding eye model and remaining constant in the models with constant linear blur (Appendices B and C; Tables 1 and 4).

Chick

The uniform expansion of the chick eye occurred with a t50 of 46 days. The scaling value, *m,* for chicks reached a value between 1.2× and 1.3× on day 14 compared to day 0. Resulting predictions of the uniformly scaled and constant linear blur models for chicks are shown in Figures 2–4 and in Tables 1–4. For the eye model with constant linear blur, EB and other absolute image quality metrics will reduce exponentially with the t50s shown in Tables 2 and 3.

Monkey

Eye expansion occurred at a t50 of 196 days (Qiao-Grider et al., 2007). The scaling value, *m,* used in the monkey eye reached a value of 1.3× on day 1500 compared to day 20 (Qiao-Grider et al., 2007). Resulting predictions of the uniformly scaled and constant linear blur models for monkeys are shown in Figure 5 and in Tables 1–4. For the constant linear blur model, the area under the MTF would be expected to improve as the square of the 1.2 times increase in pupil diameter between 23 days and 4–5 years of age. Values of the MTF area at these ages were compared (Ramamirtham et al., 2006; Appendix C, Table 3).

Human

Axial length expansion occurred at a t50 of 584 days (Qiao-Grider et al., 2007). HO RMSA and the geometric linear blur on the retina are predicted to increase exponentially in a uniformly expanding model and remain constant in the model with constant linear blur. Given the change in ocular size by a factor (*m*) of 1.5× from the human infant to adult, Wang and Candy (2005) have predicted the increase of 1.5× in HO RMSA from a uniformly expanding eye model. We add predictions of the angular and linear blurs, a metric of the PSF on the retina, and predictions of the model with constant linear blur (Tables 1–4).

Schematic eye models of the developing chick

For symmetric, schematic eye models, HO RMSA consists solely of SA. The HO RMSA in the chick schematic eye models increased monotonically as a function of age. The rate of this increase in HO RMSA was substantially faster than the uniformly scaled eye

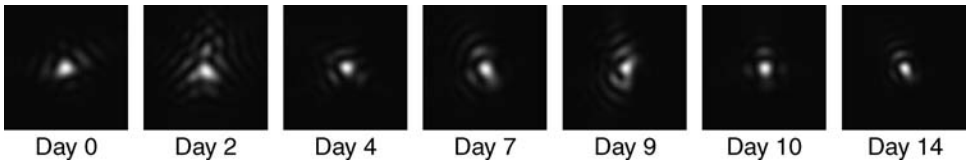

Figure 1. Angular point spread functions (PSFs) due to HOA alone (13.6 arcmin across each image) with increasing age for a sample chick eye. The PSFs are normalized to a peak intensity of 1 (white); black is zero intensity. PSFs improve (are smaller) with age. The impact of HOA is visible at day 0. Both relative and absolute image quality metrics (Figure 3) of total quality and that due to HOA improved with growth. The rates of change of the absolute image quality metrics are given in Table 3.

model. Both predict that image quality deteriorates with age (Figure 4).

Optical image quality measured in the developing eye

Chick

HO RMSA did not change significantly during development (Kisilak et al., 2006; Figure 2a) but showed a non-significant decrease with a t50 of 47.5 days. Given the rates of change of HO RMSA and pupil radius, EB due to overall HO RMSA reduced significantly exponentially with a t50 of 21.7 days and its third-order and fourth-order components also reduced exponentially with age (Figures 2c and 2d, Table 2).

The PSFs (Figures 1 and 2) and MTFs due to HOA and their metrics (Figure 3) showed rapid improvements (PSFs are smaller; MTFs are more voluminous) with increasing age (Table 3), consistent with the behavior of EB (Appendix E).

Monkey

The observed decrease in HO RMSA and linear retinal blur in growing monkeys (Ramamirtham et al., 2006) with a t50 between 18 and 41 days (for fits of the published data up to 200 days or 1500 days, respectively) indicates retinal image quality improvement (Tables 1 and 4). For coma and SA fit up to 200 days, t50s were more rapid and slower, respectively. EB has a similar t50 to HO RMSA (Figure 2b, Table 2). Areas of MTFs due to HOA calculated for a constant *f*-number showed a substantial improvement between infant and older monkeys (Ramamirtham et al., 2006; Table 3).

Human

HO RMSA in infants (Wang & Candy, 2005) was 87% of the adult value, giving adult values of HO RMSA and linear retinal blur 1.15× larger than the infant value (Tables 1 and 4). Given this result and the pupil scaling of 1.5× from infant to adult, the angular EB on the retina (Equation A1) in the adult eye will be 77% of the value in the infant eye (Table 2). PSF and MTF due to HOA improved from infant to adult with the metric PSF equivalent width (Thibos, Hong, Bradley, & Applegate, 2004) improving significantly to 76% of the infant value (Table 3), consistent with the results given by EB (Appendix E).

Experimental results compared to theoretical predictions

Chick

The variation in SA (HO RMSA) predicted by the schematic eye models of the developing chick as a function of age show an increase (decrease in image quality) that is more rapid than that of the uniformly scaling eye model and does not agree with the measured decrease in SA (increase in image quality; Figure 4).

The non-significant change in HO RMSA during development was in agreement with the constant linear blur model (Figure 2a, Table 1). However, the reduction of EB with age was more rapid than the envelope of predictions from the constant linear blur model (Figure 2b, Table 2) and consistent with an overall decrease in HO RMSA. However, if the components of HOA are considered, the experimental decrease of third-order EB was not significantly different from the envelope predicted by the constant linear blur model (Figure 2c), consistent with constant linear retinal blur due to asymmetrical aberrations. On the other hand, the experimentally determined time constant for the reduction in EB due to fourth-order RMSA was significantly faster than the envelope of predictions from the model with constant linear blur (Figure 2d, Table 4).

The improvements with growth of relative image quality metrics calculated from the PSF and the MTF of total quality and that due to HOA are inconsistent with the constant linear blur model's prediction of constancy. The exponential improvements in the absolute image quality metrics in real (Figure 3a, Table 3) and frequency (Figure 3b, Table 3) spaces are also faster than the predictions of the constant linear blur model.

Monkey

A decrease is observed in HO RMSA in growing monkeys (Ramamirtham et al., 2006) where the uniformly

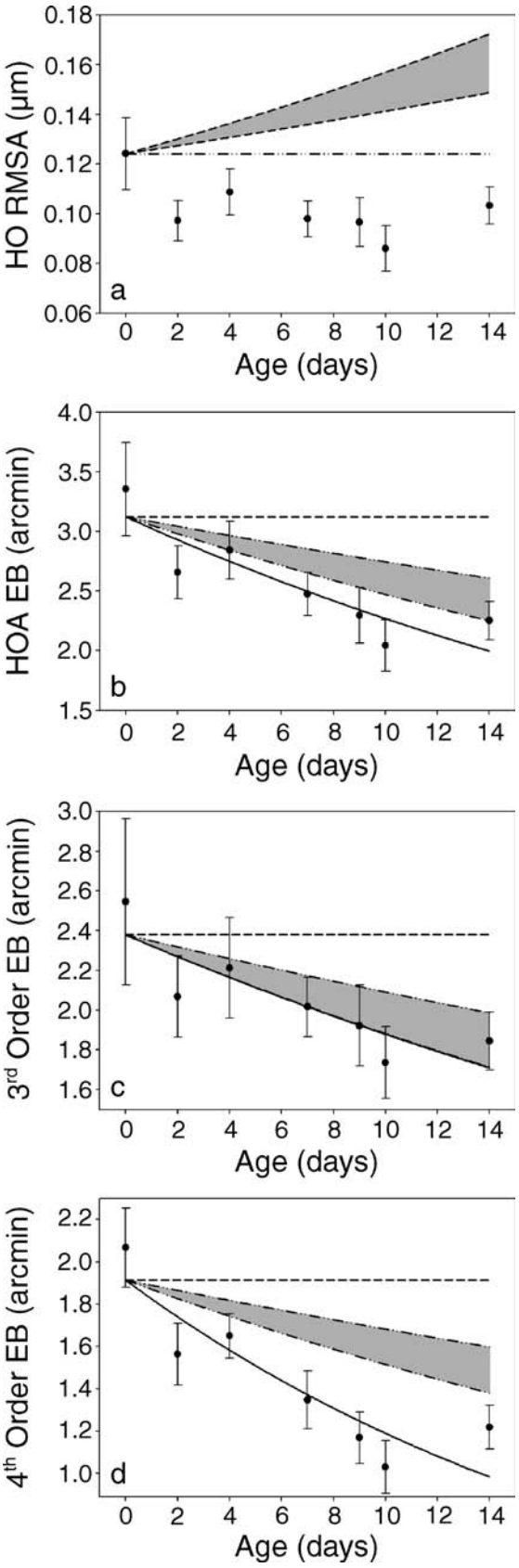

expanding model predicts an increase and the constant linear blur model predicts constancy (Figure 5a, Table 1). EB due to HOA and MTF area have faster improvements than the predictions for either the uniformly expanding or the constant linear blur models (Figure 5b, Tables 2 and 3). Coma decreased faster and SA more slowly than HO RMSA, but image quality due to these aberrations also improves with growth, faster than predicted by either eye model.

Human

HO RMSA in adult was 1.15× the infant value rather than the 1.5× predicted by uniform expansion (Wang & Candy, 2005; Table 1). This smaller increase is not significantly different from the constancy in HO RMSA predicted from our model with constant linear retinal blur.

The angular EB on the retina of the adult eye is calculated to be 77% of that in the infant eye, rather than the constancy predicted by the uniformly expanding model. Although larger than the decrease to 67% predicted by the model with constant linear retinal blur, the experimental and model results were not significantly different (Table 2). The linear retinal blur is estimated to be 15% larger in the adult eye, smaller than the 50% increase predicted by the uniformly expanding model and not significantly different from the constancy predicted by our new model (Table 4).

Improved MTFs and PSFs due to HOA were seen in the adult compared with the infant eye (Wang & Candy, 2005). An exact diffraction calculation for the uniformly scaled model is likely to show a small improvement due to the reduced effects of diffraction at the larger pupil. The substantial significant improvement observed in the metric PSF equivalent width (24%) is closer to the prediction of a 33% improvement by the model with constant linear

Figure 2. Experimental higher-order RMS aberrations (HO RMSA) and equivalent blur (EB) due to HOA across growing pupils are plotted versus chick age (days; closed circles). The error bars represent the standard errors of the experimental data. Significant exponential fits to the data (—; replotted from Kisilak et al., 2006) are shown along with the envelopes (shaded regions) of the uniformly scaled (– – –) and constant linear blur model (–·–) predictions. (a) Uniform scaling (envelope shown as shaded region) and constant linear blur models predict that HO RMSA should increase by the ocular scaling factor with age or remain constant, respectively. (b) EB due to HOA decreased with age at a rate that was significantly faster than the lower edge of the envelope (shaded region) for the prediction from the constant linear blur model and inconsistent with the uniformly scaled model's prediction of constancy. (c) For third-order EB, the lower envelope (shaded region) of the constant linear blur model prediction overlaps the best fit to the experimental data but (d) the fourth-order data decrease significantly faster than either model's prediction.

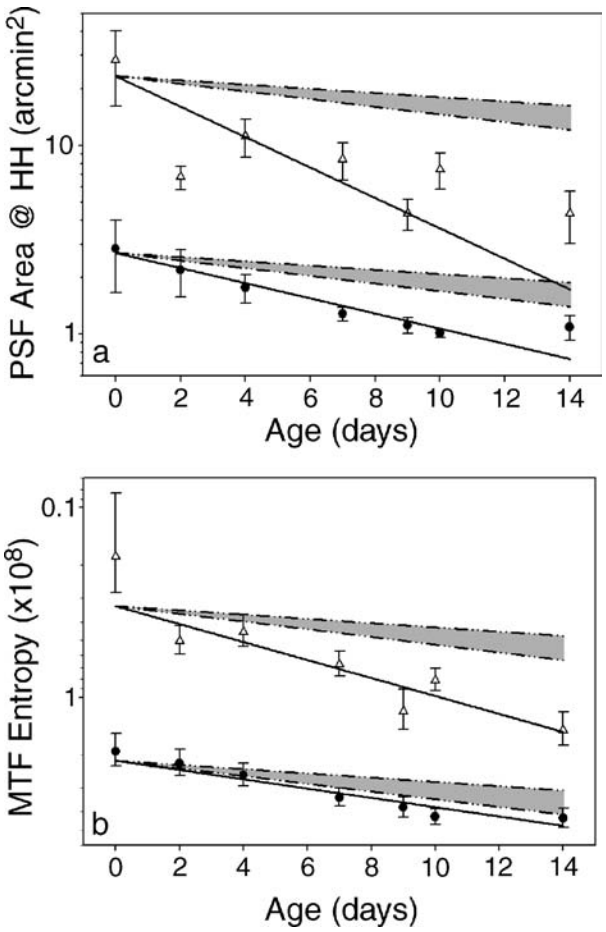

Figure 3. Comparison between the experimental variation in (a) PSF area at half-height and (b) MTF entropy with age and the envelopes (shaded region) of predictions of improvement from the constant linear blur models of eye growth (–··–). The open triangles represent second-order aberrations and up, while the closed circles are for HOA alone. Since MTF entropy increases with improving image quality, it was plotted in reverse. Exponential regressions and the model's predictions appear linear on this log scale. Image quality due to HOA and total blur improve faster than the model's predictions. A uniformly scaled model would predict even less improvement in image quality (Table 3).

retinal blur than to a uniformly expanding model. Furthermore, the standard deviations on the infant and adult values encompass a value of 33% as predicted by the model with constant linear retinal blur (Table 3).

Discussion

Models of eye growth

The two wavefront eye models discussed are equivalent to scaling the wavefront upwards (uniform model) or holding it fixed (non-uniform model) within a pupil that scales upwards with age at the same rate as the distance to the focus near the retina. Our predictions of MOR, HO RMSA, and angular retinal blur from uniformly scaled optical eye models for chicks (Kisilak et al., 2005) and monkeys are similar to those of Wang and Candy (2005) for humans. Additionally, we analyzed the EB on the retina and the linear retinal blur. We have also predicted optical changes during eye development using a novel model of growth with constant linear retinal blur in chicks (Hunter et al., 2006) and have developed this model for growing monkey and human eyes. The near constancy of HO RMSA in this new model, rather than suggesting little change in optics, suggests stretching of the wavefront error within a growing pupil with no change in phase. Although the outcome of constant HO RMSA is simple, the mechanisms that produce it would be more complex (see discussion of mechanisms).

Both wavefront models assume that the *f*-number remains constant with growth, the pupil and focal length scale at the same rate. This is a good approximation for broiler chicks as the focal power (Irving et al., 1996; White Rock) and mean pupil diameters (Kisilak et al., 2006; Ross Ross) give a change in *f*-number with age close to zero (11%). In humans, pupil size and axial length scaled similarly (Wang & Candy, 2005). In monkeys, HO RMSA was calculated while assuming pupil size scaled with axial length (Ramamirtham et al., 2006). A direct age-related pupil measurement would test the validity of the assumption in monkeys.

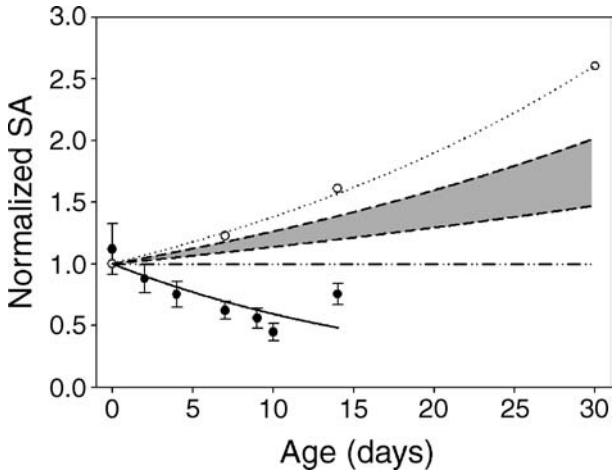

Figure 4. The best fit (—) to experimental spherical aberration (SA) versus chick age (closed circles; replotted from Kisilak, 2005) decreases with age contrary to predictions of an increase (best fits to the schematic eyes (···) and the envelope (shaded region) of the uniformly scaled model (– – –)) and constancy (non-uniformly scaled model (–··–)). The error bars represent the standard errors of the experimental data. The schematic eyes predict a faster increase in SA than the uniformly scaled model (shaded region).

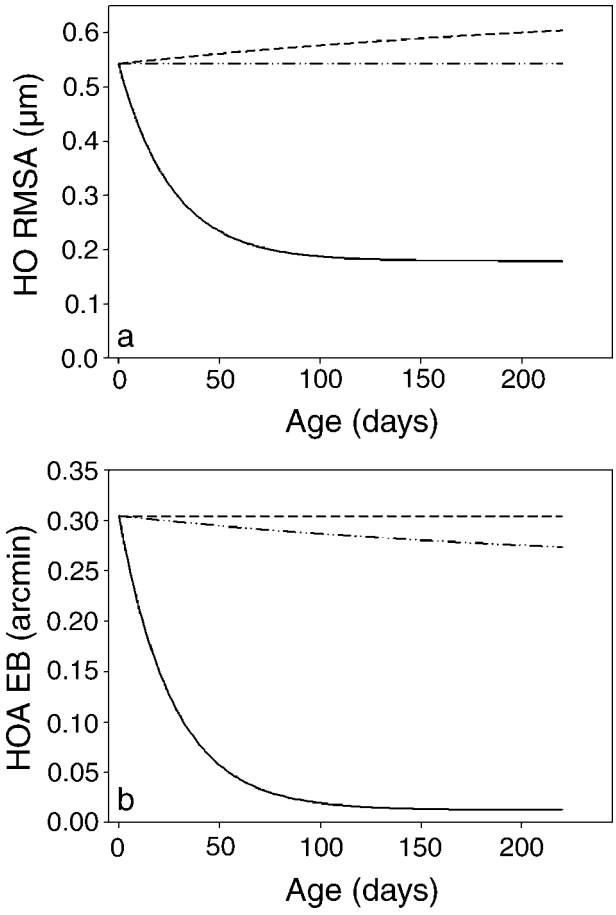

Figure 5. Higher-order RMS aberrations (HO RMSA) and equivalent blur (EB) due to HOA across growing pupils are plotted versus monkey age (days). Significant exponential fits to experimental data (—) for monkey (Ramamirtham et al., 2006) are shown along with the uniformly scaled (– – –) and constant linear blur model (–·–) predictions. (a) Uniform scaling and constant linear blur models predict that HO RMSA should increase by the ocular scaling factor with age or remain constant, respectively, while the observed HO RMSA decreased. (b) EB due to HOA decreased with age at a rate that was significantly faster than the prediction from the constant linear blur model and inconsistent with the uniformly scaled model's prediction of constancy.

In contrast to the wavefront models, biometry in monkeys and humans (Qiao-Grider et al., 2007; Zadnik et al., 1995) indicates a lack of uniform ocular scaling and meridional asymmetry (Ramamirtham et al., 2006). Nonetheless, uniformly scaled models may provide insight into underlying mechanisms of image quality changes with growth. Moreover, in chicks, age changes in optical quality due to HOA of both scaled models agree better with observed changes than age-dependent schematic eye models (with spherical surfaces). In addition to their lack of asymmetrical aberrations, the schematic eye models used here do not incorporate any surface asphericities and hence are poor predictors of the age change in spherical aberration observed in living chick eyes. More precise optical modeling would require accurate age-dependent measurements of surface asphericities, asymmetries, ocular component alignment, and the crystalline lens gradient of refractive index (GRIN), which are challenging to obtain with the required precision in small, young eyes. Alternatively, a more general wavefront model could be developed.

Comparison of wavefront model predictions and experimentally determined retinal image quality

Across species

Wavefront models, which grow exponentially for all three species, predict image quality, which when not constant, changes exponentially with age. The longitudinal experimental data for chick and monkey, when not constant, improved, also exponentially. However, uniformly scaled eye growth does not predict the observed change in HO RMSA or accurately predict the t50s of the experimental improvement in image quality metrics (due to HOA) in developing chick, monkey, or human eyes. Therefore, we confirm for chicks that more than a simple uniform expansion of the eye occurs during normal development (Kisilak et al., 2006), as previously found in monkeys (Qiao-Grider et al., 2007) and humans (Wang & Candy, 2005).

In order to maintain constant HO RMSA as observed with age (chick and human), or reduce angular retinal blur from HOA with growth (chick, monkey, and human), the shape and possibly the alignment of the anterior optics of the eye must change, reducing the blur below that in a uniformly scaled eye.

Chick

While the decrease in HO RMSA is not significant, a decrease is consistent with other relative and absolute metrics of angular image quality. These improve faster than the constant linear blur model (Figures 2b and 3). This is consistent with the previous result that, for constant pupil diameters, image quality improved faster than a uniformly expanding model of eye growth (Kisilak et al., 2006). Collectively, the results imply that angular and linear retinal image qualities due to HOA improve with age beyond the decreasing impact of diffraction.

Monkey

The published decrease in HO RMSA, the improvement in the corresponding MTF (Ramamirtham et al., 2006), and the calculated decrease in EB due to HO RMSA in growing monkeys indicate retinal image quality improvement at a rate faster than the prediction of the model with

constant linear retinal blur. Thus, the linear retinal blur due to HO RMSA decreases with age.

Human

Non-significant changes with age in HO RMSA (Wang & Candy, 2005) and linear retinal blur are consistent with our new model. The observed improvement with age in angular retinal blur (Wang & Candy, 2005) encompasses the change predicted by the model. Thus, in humans, HO RMSA and angular blur due to HOA with growth are consistent with our model of constant linear retinal blur between infant and adult.

Components of higher-order retinal blur with increasing age

In humans, the relative rates of change of differing aberration components with growth are unpublished. The time courses of different elements of retinal blur differ within and between species (chick and monkey). In chicks, in the presence of second-order aberrations and higher, PSF area at half-height and MTF entropy improved with growth similarly to blur due to MOR (Kisilak et al., 2006) but at a different rate than these blur metrics for HOA (Figure 3). Angular blur due to third-order aberrations decreased in a manner consistent with constant linear retinal blur, while fourth-order aberration blur decreased more rapidly (Figures 2c and 2d). In contrast, in monkeys, coma (third-order) decreased more rapidly than spherical aberration (fourth-order; Ramamirtham et al., 2006) and the blur from both decreased more rapidly than predicted by the model.

A difference in time course among HOA types is not surprising because symmetrical (fourth-order) aberrations are impacted by surface curvatures and their asphericities, while asymmetrical (third-order) aberrations are altered by optical component asymmetries and alignment. In contrast to Howland's (2005) equation, the relative contributions of symmetric and asymmetric aberrations to image quality in chicks vary with age (Kisilak et al., 2006), altering the shape of both the constant and varying pupil PSFs (Figure 1) and giving an age dependence of the constant pupil wavefront error.

Mechanisms of constant or decreasing HO RMSA and decreasing angular blur during ocular growth

Our results show that the age change in linear retinal blur is species dependent. The linear retinal blur due to HOA in humans and to third-order HOA in chicks (and the corresponding HO RMSA) are approximately constant with age. Overall linear blur (and HO RMSA) in chicks and monkeys decrease with age. Uniform ocular expansion worsens aberrations and cannot explain the improvements in image quality with age. Hence, more complicated optical changes are required to produce the observed results. Possible mechanisms of constant HO RMSA within the growing pupil (Movie 2; Campbell, Hunter, Kisilak, & Irving, 2008) include an age-independent linear accuracy of optical alignment and/or surface shapes. Constant linear deviations from perfect shapes could give constant HO RMSA. This could represent either passive non-uniformities or an accuracy limit within an active, feedback mechanism during component growth. On the other hand, wavefront defects within the smaller pupil at a young age may passively impact the overall HO RMSA progressively less as the eye grows, giving decreasing HO RMSA.

Constant linear misalignment of the optical elements could passively cause a decrease in the angular misalignment of ocular components with age and a more constant wavefront error, in contrast to the increase predicted by uniform expansion. To our knowledge, there have been no measurements of the alignment of the optical surfaces or angle lambda in the chick or monkey eye during eye growth. In humans, crystalline lens tilt decreases with age (Hu, Jian, Cheng & Hsu, 2006). Alternatively, a constancy of the posterior pole geometry, as suggested with growth (De Silva et al., 2006; Larsen, 1971) and across refractive errors (Tabernero, Benito, Alcon, & Artal, 2007) in humans, could passively give a decreasing angle between the area centralis and optical axis and would give more constant aberrations compared to those in uniform scaling with a constant angular distance. A decreasing angle lambda with growth is seen in humans (Riddell, Hainline, & Abramov, 1994).

A decreasing angular distance of the fovea to the optical axis and thus more constant linear blur would be suggested in monkeys by the constancy of posterior pole geometry seen *in vitro* (Packer, Hendrickson, & Curcio, 1990). However, Quick and Boothe (1992) suggested that angle lambda and the Hirschberg ratio in monkeys do not change as a function of age and this would be expected to give increasing linear retinal blur. Thus, the decrease in linear retinal blur in monkeys with age is surprising and may be due to improved quality of the optics independent of foveal position. The mechanisms for improving image quality discussed could be active or passive, or a combination of both.

The decrease in the amount of angular retinal blur with age, observed in each of the three species, could be driven actively by an improving visual system sensitivity to blur through a number of possible mechanisms. Firstly, if retinal linear sampling remained constant, then angular sampling would improve during growth. This could be true if there were little or no expansion of the retina in the area centralis, as found in monkeys (Packer et al., 1990) and postulated in growing (Larsen, 1971) and myopic humans (Atchison et al., 2004) or if there is little change in central retinal ganglion cell density, as found in chicks (Straznicky & Chehade, 1987) (in spite of an overall

decrease in ganglion cells (Chen, Wang, Shibata, & Naito, 2004)). Alternatively, the cones and other retinal sampling elements at the visual axis may increase in numbers, giving increased angular sensitivity due to cone migration as the eye grows in humans and monkeys (Chen & Naito, 1999; Hendrickson & Yuodelis, 1984; Packer et al., 1990; Springer & Hendrickson, 2005; Yuodelis & Hendrickson, 1986). This increase in sampling could counteract retinal stretching and even improve sampling with age in order to adequately sample the improving angular blur. Thirdly, cones continue to develop with age in primates (Hendrickson & Drucker, 1992; Lopez, Lopez-Gallardo, Busturia, Anezary, & Prada, 2005; Narayanan & Wadhwa, 1998) and differentiation of oil droplets and presumably cones is complete in the chick between hatching and day 15 (Lopez et al., 2005), potentially giving improved cone sensitivity to retinal blur. If any of these mechanisms give linear retinal sensitivity to blur, which is constant or improving with age, the angular extent of retinal blur could decrease via feedback mechanisms from the retina to the optics (Kelly et al., 2004; Kröger et al., 2001).

Defocus and HOA retinal blur during eye growth

Although defocus emmetropizes primarily through eye length changes (Irving et al., 1991; Qiao-Grider et al., 2007; Schaeffel et al., 1988), a scaled model of growth is still a good approximation of the paraxial optics for the species considered. This is because the fine-tuning of ocular length required to reduce the refractive errors during normal growth is much smaller than the overall change in eye size.

The anterior segment changes necessary for constant linear blur in humans or decreasing linear blur in chicks and monkeys could occur either through passive mechanisms or retinal controlled changes, unrelated to the tuning of length. In chicks and monkeys, defocus and HOA blurs have different rates of change (Figure 3 for chick) and HO RMSA in monkey decreases at a rate faster than the increase in eye length or corneal radius (Ramamirtham et al., 2006, 2007). Thus changes in aberrations in normal monkeys and chicks do not appear to be secondary to defocus emmetropization.

In chicks and monkeys, the retinal blur due to HOA decreased with age faster than a model with either uniform expansion or constant linear retinal blur and these decreases were interrupted by lens treatment (Kisilak et al., 2006; Ramamirtham et al., 2007). Third-order aberrations increased soon after goggling in chick eyes undergoing lens induction of myopia and subsequently reduced at a rate different from that of refractive error emmetropization to the goggle power (Kisilak et al., 2006). This is consistent with individual compensation and fine-tuning of coma in humans (Kelly et al., 2004). In monkeys, both trefoil and spherical aberration changed in response to lenses (Ramamirtham et al., 2006). These results suggest the possibility of an active emmetropization of some HOA components in chick and monkey eyes.

Extension of models

Retinal and visual system changes with growth

The retinal blur may match the visual system sensitivity to blur from a young age. In this case, a change in retinal sensitivity to linear blur as a function of age could be predicted from the difference between the constant linear blur model prediction and the actual decrease in image quality. Differences among species in the rate of decrease in image quality could result from a mismatch of blur to sensitivity at a young age, from differing initial relative amounts of defocus and HOA blurs or from differing age changes in visual sampling and/or sensitivity (Bumsted & Hendrickson, 1999; Hendrickson, 1992).

Other species and ages

The constant linear blur model developed here could predict changes in optical quality during normal development in other species, provided that ocular growth can be approximated by a scaling function. Data are available for many animals that emmetropize, including older chicks (Schaeffel & Howland, 1988), humans (Qiao-Grider et al., 2007), marmosets (Coletta, Troilo, Moskowitz, Nickla, & Marcos, 2004; Graham & Judge, 1999), tree shrews (Norton & McBrien, 1992), guinea pigs (Howlett & McFadden, 2007), and the rat, for which there is not yet convincing evidence of emmetropization (Guggenheim, Creer, & Qin, 2004). Corresponding image quality measurements would be required for a comparison between the model and the experimental data.

Myopic eye growth

Image quality changes during the induction of myopia in human and animal models might also be predicted from analogous models of eye growth. In young chicks wearing −15D goggles, there is an initial delay and a subsequent reduction of HOA with growth (Kisilak et al., 2006). Chick aberrations were not proportional to the duration of myopia induction, nor were they monotonic with the amount of myopia induced (Kisilak et al., 2006). These longitudinal optical quality measurements (Kisilak et al., 2006) suggest complex ocular changes in response to goggling. Length changes could contribute (without any optical component changes) to aberration changes (Cheng, Bradley, Hong, & Thibos, 2003), but our analysis of chick eye models suggest that this does not occur in chicks (Hunter, 2006). Ignoring aberration changes with eye length, a goggled eye may initially scale uniformly in size,

leading to a delay in the decrease in HOA EB in the goggled eye relative to the control (Kisilak et al., 2006). The subsequent decrease in HOA EB (Kisilak et al., 2006) indicates that the linear blur due to HOA on the retina decreases with age even as the eye continues to grow in response to the goggle. This further indicates that changes in HOA are not secondary to myopia induction.

Conclusions

Rates of ocular component growth can be used to predict changes in optical quality on the retina with normal development according to two relatively simple models of the behavior of wavefront aberrations. One model uniformly scales with growth, while the second, new model holds linear blur constant on the retina. Consequently, wavefront aberration, normalized to the pupil radius, is also constant with growth. Predictions of image quality from HOA given by these simple models are superior to those of schematic eye models with spherical surfaces. Comparison of wavefront model predictions with experimentally measured changes in wavefront aberrations and resulting retinal blur for chicks, monkeys, and humans showed that, in all three species, the observed improvement in angular blur due to HOA is more rapid than the constancy given by uniform ocular expansion. Thus, the shape and/or angular alignment of the anterior optics of the eyes must change with growth.

In chicks, blur due to third-order aberrations and, in humans, total blur due to HOA decreased at a rate consistent with the model with constant linear retinal blur. These results could be explained by constant wavefront error caused by an age independence of linear optical alignment accuracy or a reducing angle of the area centralis to the optical axis. In chicks and monkeys, linear retinal blur due to HOA decreases with age. Thus, the age change in linear retinal blur is species dependent, as are changes in the retina with age, which could influence visual sensitivity to retinal blur. Furthermore, in chicks, the asymmetric component of retinal blur and in monkeys, symmetrical and asymmetrical components decreased with age faster than uniformly scaled model predictions and these decreases were interrupted by lens treatment (Kisilak et al., 2006; Ramamirtham et al., 2007). This and the difference between the rate of decrease in aberration blur and the rates of eye growth and the emmetropization of defocus suggest that HOA changes are not secondary to either overall growth or defocus changes. They are potentially consistent with emmetropization of some aberration components. Comparison of aberration measurements with model predictions provides insight into growth changes in the ocular optics and the potential role of HOA in emmetropization and refractive error development.

Appendix A

Metrics of ocular image quality

There are several ways to evaluate image quality. HO RMSA wavefront error is a well-established metric that describes wavefront changes normalized in the pupil relative to the diffraction limit. Relative image quality metrics compare properties at a given pupil size to the diffraction limit. Absolute image quality metrics take into account the size of the PSF or OTF in real or frequency space as a function of changing pupil size with growth. Metrics of image quality can either be directly measured or derived from knowledge of the HOA (Thibos, Hong, Bradley, & Cheng, 2002). Absolute changes in retinal image quality with age and with pupil size changes were approximated by the angular metric, equivalent blur (EB; Kisilak et al., 2006), which is simple to calculate, incorporates pupil size, and approximates the geometrical angular blur on the retina:

$$\mathrm{EB} = \frac{\mathrm{RMSA}}{\text{pupil radius}}. \quad \text{(A1)}$$

It differs from equivalent defocus (Thibos, Hong et al., 2002) by a factor of the pupil radius. Other absolute image quality metrics used here for chick include measures of the extent of the point spread function (PSF), specifically its area at half-height and the entropy of the modulation transfer function (MTF). The relative metrics, Strehl ratio and the ratio of the volume of the OTF to the volume of the MTF, were also calculated. The absolute and relative metrics presented for chick are representative of the behavior of a number of metrics (Hunter, 2006). The metrics discussed for monkey and human were those for which literature values were available or which could be calculated.

Appendix B

A model of uniformly scaled eye growth

In a uniformly scaled model, all optical parameters are equally magnified by a factor (m) and the f-number remains constant with growth (Howland, 2005; Kisilak et al., 2006; Wang & Candy, 2005). As a consequence, the linear retinal blur from wavefront aberrations (transverse aberration) will scale by m (Smith, 2000). The corresponding Zernike coefficients, describing the wavefront aberration and the root mean square of the wavefront aberration (RMSA) will also increase by the scaling factor (Kisilak et al., 2005; Wang & Candy, 2005). The scaling factor will depend on observed changes in the optics of the eye and will be a function of age. Equivalent blur

(Equation A1) will remain constant with uniformly scaled growth, while mean ocular refraction (MOR) and equivalent defocus (Thibos, Hong et al., 2002) will decrease as $1/m$. The linear blur on the retina in an emmetropic eye can be estimated by multiplying the EB by the posterior nodal distance (PND). The PND is the distance between the posterior nodal point and the posterior focal point. This is equal to the anterior focal length of the eye. For growing, normal eyes, the PND is very nearly equal to the nodal point to retina distance, which should be used in an exact calculation. In this uniformly scaled model, the linear retinal blur will scale as m.

Both the linear blur on the retina and its angular projection into object space (angular blur, Movie 1) may change with growth, both from changes in aberrations and from the decreasing diffraction from increasing pupil size. If the impact of diffraction is considered, the angular extent of the Airy disc (aberration-free PSF) will decrease by $1/m$ and the linear extent will be constant with uniform scaling. This introduces two limits for the prediction of changes in the overall PSF size with scaling. In the presence of negligible aberrations, the effect of diffraction will dominate and the angular PSF will decrease in size. When the aberrations are large, the geometrical blur will dominate and the angular PSF will not change with uniform scaling. Between these limits, the scaling of the PSF will be more complicated. As such, predictions with growth for changes in PSF- and OTF-derived metrics of image quality will have a complex dependence on m.

If the wavefront aberration of a given order is analyzed across a constant pupil diameter while the eye is undergoing uniformly scaled growth, each normalized wavefront aberration term and its RMS will depend on the inverse of the scaling factor raised to a power of its Zernike order less one (Howland, 2005; Kisilak et al., 2005), $1/(m^{\text{order}-1})$. The EB and equivalent defocus (Thibos, Hong et al., 2002) will each have the same relationship as the RMSA. Thus, all image quality metrics will also depend on the orders of the Zernike coefficients involved. Because the change in wavefront aberration is dependent on the order of the Zernike terms being considered, if more than one order is used, then the prediction for a constant pupil diameter is complicated and will depend on the relative contributions of each Zernike order involved.

Appendix C

A model of non-uniformly scaled ocular growth with constant linear retinal blur

In the constant linear blur model, paraxial properties, pupil, and eye size are magnified by the scaling factor (m), but the transverse aberration and the linear extent of the diffraction blur on the retina both remain constant (Hunter et al., 2006). Thus, the wavefront aberrations in the pupil and their RMSA must remain constant. As such, EB (Equation A1) will decrease by $1/m$ as the eye increases in size. Angular diffraction blur will decrease at the same rate. The overall angular PSF width will scale as $1/m$ and the overall angular OTF width will scale as m. Metrics of the PSF and OTF relative to the diffraction limit will remain constant with the constant linear blur model, while absolute metrics improve. For this constant linear blur model, absolute linear metrics like PSF equivalent width (Thibos et al., 2004) will improve as $1/m$ while absolute area metrics like PSF area at half-height varies as $1/m^2$ and MTF area or entropy varies as m^2.

Appendix D

Calculation of the rates of change of image quality in the developing eye

Chick

For this age range, experimental data for HO RMSA and pupil size variations were each well fit with an exponential function (Kisilak, 2005; Kisilak et al., 2006) so that

$$\text{HO RMSA} = \text{RMSA}_0 \exp\left[-\frac{\text{day}}{\tau_{\text{RMSA}}}\right], \tag{D1}$$

$$\text{Pupil radius} = p_0 \exp\left[\frac{\text{day}}{\tau_P}\right], \tag{D2}$$

where RMSA_0 and p_0 are the initial values of HO RMSA and pupil radius, respectively, and τ_{RMSA} and τ_P are the time courses of HO RMSA and pupil radius, respectively.

Then, equivalent blur (EB) is

$$\text{EB} = \frac{\text{HO RMSA}}{\text{Pupil radius}}, \tag{D3}$$

$$\text{EB} = \frac{\text{RMSA}_0 \exp\left[-\frac{\text{day}}{\tau_{\text{RMSA}}}\right]}{p_0 \exp\left[\frac{\text{day}}{\tau_P}\right]}, \tag{D4}$$

$$\mathrm{EB} = \frac{\mathrm{RMSA}_0}{p_0} \exp\left[-\mathrm{day}\left(\frac{1}{\tau_{\mathrm{RMSA}}} + \frac{1}{\tau_P}\right)\right], \tag{D5}$$

$$\mathrm{EB} = \frac{\mathrm{RMSA}_0}{p_0} \exp\left[-\frac{\mathrm{day}}{\tau_{\mathrm{EB}}}\right]. \tag{D6}$$

Thus, the time constant of EB is given by

$$\frac{1}{\tau_{\mathrm{EB}}} = \frac{1}{\tau_{\mathrm{RMSA}}} + \frac{1}{\tau_P}. \tag{D7}$$

The time to a 50% increase in eye size from the initial value (t50) is related to τ by

$$\mathrm{t50} = \frac{\ln 2}{\tau}. \tag{D8}$$

Time courses are given in Table 1 for the two models and the observed data. In the uniformly expanding eye model, where the HO RMSA varies with the same time constant as the pupil,

$$\frac{1}{\tau_{\mathrm{RMSA}}} = \frac{-1}{\tau_P}, \tag{D9}$$

so that

$$\frac{1}{\tau_{\mathrm{EB}}} = 0, \tag{D10}$$

and EB is constant. In the model with constant linear retinal blur, HO RMSA is constant and EB declines with the same t50 as the variation of pupil size.

For both model and experiment, the linear retinal blur (LRB) is calculated as the EB times the focal length of the eye (f). If the focal length scales exponentially (Carroll, 1982) with a time constant of τ_f from an initial value f_0, then,

$$\mathrm{LRB} = \mathrm{EB} * \text{focal length}, \tag{D11}$$

$$\mathrm{LRB} = \left\{\frac{\mathrm{RMSA}_0}{p_0} \exp\left[-\mathrm{day}\left(\frac{1}{\tau_{\mathrm{RMSA}}} + \frac{1}{\tau_P}\right)\right]\right\} \times \left\{f_0 \exp\left[\frac{\mathrm{day}}{\tau_f}\right]\right\}, \tag{D12}$$

$$\mathrm{LRB} = \frac{\mathrm{RMSA}_0 f_0}{p_0} \exp\left[-\mathrm{day}\left(\frac{1}{\tau_{\mathrm{RMSA}}} + \frac{1}{\tau_P} - \frac{1}{\tau_f}\right)\right], \tag{D13}$$

$$\mathrm{LRB} = \frac{\mathrm{RMSA}_0 f_0}{p_0} \exp\left[-\frac{\mathrm{day}}{\tau_{\mathrm{LRB}}}\right], \tag{D14}$$

where

$$\frac{1}{\tau_{\mathrm{LRB}}} = \frac{1}{\tau_{\mathrm{RMSA}}} + \frac{1}{\tau_P} - \frac{1}{\tau_f}. \tag{D15}$$

When the f-number ($f\#$ is equal to the focal length divided by the pupil radius) is constant with age, $\tau_P = \tau_f$ and $\tau_{\mathrm{LRB}} = \tau_{\mathrm{RMSA}}$ so that

$$\mathrm{LRB} = f\#\,\mathrm{RMSA}_0 \exp\left[-\frac{\mathrm{day}}{\tau_{\mathrm{RMSA}}}\right], \tag{D16}$$

indicating that the time constants for both HO RMSA and LRB are equal.

Monkey

The experimental values given for HO RMSA and pupil size (scaled as eye length; Ramamirtham et al., 2006) out to day 1500 were well fit with exponentials, which in the cases of HO RMSA and pupil size, declined to a minimum and increased to a maximum, respectively. Thus

$$\text{HO RMSA} = (\mathrm{RMSA}_0 - a_{\mathrm{RMSA}}) + a_{\mathrm{RMSA}} \exp\left[-\frac{\mathrm{day}}{\tau_{\mathrm{RMSA}}}\right], \tag{D17}$$

$$\text{Pupil radius} = (p_0 + a_P) - a_P \exp\left[-\frac{\mathrm{day}}{\tau_P}\right], \tag{D18}$$

where a_{RMSA} and a_P are the change in HO RMSA and pupil radius between day 0 and the minimum and maximum values, respectively. So that

$$\mathrm{EB} = \frac{(\mathrm{RMSA}_0 - a_{\mathrm{RMSA}}) + a_{\mathrm{RMSA}} \exp\left[-\frac{\mathrm{day}}{\tau_{\mathrm{RMSA}}}\right]}{(p_0 + a_P) - a_P \exp\left[-\frac{\mathrm{day}}{\tau_P}\right]}. \tag{D19}$$

EB was then calculated from Equation D19 and was well fit with an exponential out to day 200. In addition, from values given for HO RMSA and pupil size, EB was also calculated at days 23, 200, and 1500 and these values were also well fit with an exponential.

The t50s were calculated as the duration required for a change of 50% of the difference between initial and final values, that is, a change of $a_{\mathrm{RMSA}}/2$ or $a_P/2$. The t50 of the resulting experimental EB was close to the t50 for HO RMSA because the change in HO RMSA was much more rapid than the change in pupil size:

$$\mathrm{EB} = \frac{(\mathrm{RMSA}_0 - a_{\mathrm{RMSA}})\left\{1 + \frac{a_{\mathrm{RMSA}}}{\mathrm{RMSA}_0 - a_{\mathrm{RMSA}}}\exp\left[-\frac{\mathrm{day}}{\tau_{\mathrm{RMSA}}}\right]\right\}}{(p_0 + a_P)\left\{1 - \frac{a_P}{p_0 + a_P}\exp\left[-\frac{\mathrm{day}}{\tau_P}\right]\right\}}. \quad \text{(D20)}$$

In the uniformly expanding eye model, where the HO RMSA varies with the same time constant as the pupil, $\tau_{\mathrm{RMSA}} = \tau_P$, $a_{\mathrm{RMSA}} < 0$ and the HO RMSA and pupil size show the same proportional changes from initial to final values, then EB is constant:

$$\mathrm{EB} = \frac{\mathrm{RMSA}_0}{p_0}. \quad \text{(D21)}$$

In the model with constant linear retinal blur, HO RMSA is constant and EB declines with the same t50 as the variation of pupil size.

The LRB varies as the EB times the focal length. As in the chick, since the *f*-number is constant, the focal length varies as the pupil size. Thus, as in the chick, both model and experimental LRB will vary as the HO RMSA (Table 1).

Human

The change in EB was calculated from Equation A1 for the pupil sizes assumed for constant *f*-number for infant and adult (Wang & Candy, 2005). Again, LRB will vary as the HO RMSA.

Appendix E

Variation of image quality metrics in chick and human eyes with age

For the range of RMS wavefront errors in the chick, with and without defocus, the variation of image quality metrics with RMSA were found by regression analysis of the metrics calculated for the wavefronts as a function of age (across a normalized pupil size). PSF area at half-height was found to vary as

$$\frac{\mathrm{RMSA}^2}{r^2}, \quad \text{(E1)}$$

and MTF entropy varied as

$$\frac{r^2}{\mathrm{RMSA}}. \quad \text{(E2)}$$

Although RMSA in the chick does not change significantly with age, the exponential time courses of the image quality metrics of the experimental data (Figure 2) are consistent with an exponential decrease in RMSA with age, which contributes to the metrics' improvement with age. From this analysis, EB in chick (Equation A1) varies as the square root of the PSF area at half-height. Thus EB predicts well the age variation in angular subtense of the PSF for RMS wavefront errors found in chick (up to 1.8 wavelengths including second-order errors; Kisilak et al., 2006). Furthermore, in human, the change in EB observed between infant and adult closely approximates the observed change in PSF equivalent width (Tables 2 and 3).

Acknowledgments

This research was conducted at the University of Waterloo and was supported by CFI, OPC, and NSERC, Canada. JJH was supported by an Ontario Graduate Scholarship. ELI holds a Canada Research Chair and was supported by PREA.

Commercial relationships: none.
Corresponding author: Jennifer J. Hunter.
Email: jhunter@cvs.rochester.edu.
Address: Meliora Hall, University of Rochester, Rochester, NY 14627-0270, USA.

References

Artal, P., Benito, A., & Tabernero, J. (2006). The human eye is an example of robust optical design. *Journal of Vision, 6*(1):1, 1–7, http://journalofvision.org/6/1/1/, doi:10.1167/6.1.1. [PubMed] [Article]

Atchison, D. A., Jones, C. E., Schmid, K. L., Pritchard, N., Pope, J. M., Strugnell, W. E., et al. (2004). Eye shape in emmetropia and myopia. *Investigative Ophthalmology & Visual Science, 45,* 3380–3386. [PubMed] [Article]

Brown, N. P., Koretz, J. F., & Bron, A. J. (1999). The development and maintenance of emmetropia. *Eye, 13,* 83–92. [PubMed]

Bumsted, K., & Hendrickson, A. (1999). Distribution and development of short-wavelength cones differ between Macaca monkey and human fovea. *Journal of Comparative Neurology, 403,* 502–516. [PubMed]

Campbell, M. C. W., Hunter, J. J., Kisilak, M. L., & Irving, E. L. (2008). Wavefront-based eye models for the study of developmental changes. *Frontiers in Optics,* Abstract FthA4.

Campbell, M. C. W., Priest, D., & Hunter, J. J. (2001). The importance of monochromatic aberrations to detecting defocus in retinal images. *Investigative Ophthalmology & Visual Science, 42,* 539.

Carkeet, A., Luo, H. D., Tong, L., Saw, S. M., & Tan, D. T. H. (2002). Refractive error and monochromatic aberrations in Singaporean children. *Vision Research, 42,* 1809–1824. [PubMed]

Carroll, J. P. (1982). On emmetropization. *Journal of Theoretical Biology, 95,* 135–144. [PubMed]

Charman, W. N. (2005). Aberrations and myopia. *Ophthalmic and Physiological Optics, 25,* 285–301. [PubMed]

Chen, Y., & Naito, J. (1999). A quantitative analysis of cells in the ganglion cell layer of the chick retina. *Brain, Behavior and Evolution, 53,* 75–86. [PubMed]

Chen, Y., Wang, Z., Shibata, H., & Naito, J. (2004). Quantitative analysis of cells in the ganglion cell layer of the chick retina: Developmental changes in cell density and cell size. *Anatomia, Histologia, Embryologia, 33,* 161–167. [PubMed]

Cheng, X., Bradley, A., Hong, X., & Thibos, L. N. (2003). Relationship between refractive error and monochromatic aberrations of the eye. *Optometry and Vision Science, 80,* 43–49. [PubMed]

Coletta, N. J., Troilo, D., Moskowitz, A., Nickla, D. L., & Marcos, S. (2004). Ocular wavefront aberrations in the awake marmoset. *Investigative Ophthalmology & Visual Science, 45,* 4298.

Collins, M. J., Wildsoet, C. F., & Atchison, D. A. (1995). Monochromatic aberrations and myopia. *Vision Research, 35,* 1157–1163. [PubMed]

De Silva, D. J., Cocker, K. D., Lau, G., Clay, S. T., Fielder, A. R., & Moseley, M. J. (2006). Optic disk size and optic disk-to-fovea distance in preterm and full-term infants. *Investigative Ophthalmology & Visual Science, 47,* 4683–4686. [PubMed] [Article]

Garcia de la Cera, E., Rodriguez, G., & Marcos, S. (2006). Longitudinal changes of optical aberrations in normal and form-deprived myopic chick eyes. *Vision Research, 46,* 579–589. [PubMed]

Graham, B., & Judge, S. J. (1999). Normal development of refractive state and ocular component dimensions in the marmoset (callithrix jacchus). *Vision Research, 39,* 177–187. [PubMed]

Guggenheim, J. A., Creer, R. C., & Qin, X. J. (2004). Postnatal refractive development in the brown Norway rat: Limitations of standard refractive and ocular component dimension measurement techniques. *Current Eye Research, 29,* 369–376. [PubMed]

He, J. C., Sun, P., Held, R., Thorn, F., Sun, X. R., & Gwiazda, J. E. (2002). Wavefront aberrations in eyes of emmetropic and moderately myopic school children and young adults. *Vision Research, 42,* 1063–1070. [PubMed]

Hendrickson, A. (1992). A morphological comparison of foveal development in man and monkey. *Eye, 6,* 136–144. [PubMed]

Hendrickson, A., & Drucker, D. (1992). The development of parafoveal and mid-peripheral human retina. *Behavioural Brain Research, 49,* 21–31. [PubMed]

Hendrickson, A. E., & Yuodelis, C. (1984). The morphological development of the human fovea. *Ophthalmology, 91,* 603–612. [PubMed]

Hirsch, M. J., & Weymouth, F. W. (1990). Prevalence of refractive anomalies. In T. Grosvenor & M. C. Flom (Eds.), *Refractive anomalies: Research and clinical applications* (pp. 15–38). Boston: Butterworth-Heinemann.

Howland, H. C. (2005). Allometry and scaling of wave aberration of eyes. *Vision Research, 45,* 1091–1093. [PubMed]

Howlett, M. H., & McFadden, S. A. (2007). Emmetropization and schematic eye models in developing pigmented guinea pigs. *Vision Research, 47,* 1178–1190. [PubMed]

Hu, C. Y., Jian, J. H., Cheng, Y. P. & Hsu, H. K. (2006). Analysis of crystalline lens position. *Journal of Cataract and Refractive Surgery, 32,* 599–603. [PubMed]

Hunter, J. J. (2006). Image quality in ocular development and fundus imaging (PhD, University of Waterloo).

Hunter, J. J., Campbell, M. C. W., Kisilak, M. L., & Irving, E. L. (2003). Signals to the direction of defocus from monochromatic aberrations in chick eyes that develop lens induced myopia. *Investigative Ophthalmology & Visual Science, 44,* 4341.

Hunter, J. J., Kisilak, M. L., Campbell, M. C. W., Irving, E. L., & Huang, L. (2006). Predictions of blur sensitivity improvement in the growing chick eye. *Investigative Ophthalmology & Visual Science, 47,* 3337.

Irving, E. L., Callender, M. G., & Sivak, J. G. (1991). Inducing myopia, hyperopia, and astigmatism in chicks. *Optometry and Vision Science, 68,* 364–368. [PubMed]

Irving, E. L., Sivak, J. G., Curry, T. A., & Callender, M. G. (1996). Chick eye optics: Zero to fourteen days. *Journal of Comparative Physiology A, Sensory, Neural, and Behavioral Physiology, 179,* 185–194. [PubMed]

Kee, C., Hung, L.-F., Qiao, Y., Habib, A., & Smith, E. L. (2002). Prevalence of astigmatism in infant monkeys. *Vision Research, 42,* 1349–1359. [PubMed]

Kelly, J. E., Mihashi, T., & Howland, H. C. (2004). Compensation of corneal horizontal/vertical astigmatism, lateral coma, and spherical aberration by internal optics of the eye. *Journal of Vision, 4*(4):2, 262–271, http://journalofvision.org/4/4/2/, doi:10.1167/4.4.2. [PubMed] [Article]

Kisilak, M. L. (2005). Optical aberrations in growing eyes and in eyes with lens-induced myopia (MSc, University of Waterloo).

Kisilak, M. L., Bunghardt, K., Ball, A. K., Irving, E. L., & Campbell, M. C. W. (2008). *In vivo* imaging of photoreceptors in the alert chick during development. *Investigative Ophthalmology & Visual Science, 49,* 4010.

Kisilak, M. L., Campbell, M. C., Hunter, J. J., Irving, E. L., & Huang, L. (2006). Aberrations of chick eyes during normal growth and lens induction of myopia. *Journal of Comparative Physiology A, Neuroethology, Sensory, Neural, and Behavioral Physiology, 192,* 845–855. [PubMed]

Kisilak, M. L., Hunter, J. J., Campbell, M. C. W., Irving, E. L., & Huang, L. (2005). Optical changes in normal chick eyes with age and in eyes with lens-induced myopia. *Investigative Ophthalmology & Visual Science, 46,* 1971.

Kisilak, M. L., Hunter, J. J., Huang, L., Campbell, M. C. W., & Irving, E. L. (2008). In chicks wearing high powered negative lenses, spherical refraction is compensated and oblique astigmatism is induced. *Journal of Modern Optics, 55,* 611–623.

Koretz, J. F., Rogot, A., & Kaufman, P. L. (1995). Physiological strategies for emmetropia. *Transactions of the American Ophthalmological Society, 93,* 118–122. [PubMed] [Article]

Kröger, R. H., Campbell, M. C., & Fernald, R. D. (2001). The development of the crystalline lens is sensitive to visual input in the African cichlid fish, haplochromis burtoni. *Vision Research, 41,* 549–559. [PubMed]

Larsen, J. S. (1971). The sagittal growth of the eye. 1. Ultrasonic measurement of the depth of the anterior chamber from birth to puberty. *Acta Ophthalmologica, 49,* 239–262. [PubMed]

Llorente, L., Barbero, S., Cano, D., Dorronsoro, C., & Marcos, S. (2004). Myopic versus hyperopic eyes: Axial length, corneal shape and optical aberrations. *Journal of Vision, 4*(4):5, 288–298, http://journalofvision.org/4/4/5/, doi:10.1167/4.4.5. [PubMed] [Article]

Lopez, R., Lopez-Gallardo, M., Busturia, I., Anezary, L., & Prada, C. (2005). Spatial and temporal patterns of growth and differentiation of cone oil droplets in the chick retina. *Journal of Neuroscience Research, 79,* 401–411. [PubMed]

Lotmar, A. (1976). Theoretical model for the eye of newborn infants. *Albrecht von Graefes Archiv für Klinische und Experimentelle Ophthalmologie, 198,* 179–185. [PubMed]

Marcos, S., Moreno-Barriuso, E., Llorente, L., Navarro, R., & Barber, S. (2000). Do myopic eyes suffer from larger amount of aberrations? *Proceedings of the VIII International Conference on Myopia* (pp. 118–121). Boston.

Narayanan, K., & Wadhwa, S. (1998). Photoreceptor morphogenesis in the human retina: A scanning electron microscopic study. *The Anatomical Record, 252,* 133–139. [PubMed] [Article]

Norton, T. T., & McBrien, N. A. (1992). Normal development of refractive state and ocular component dimensions in the tree shrew (tupaia belangeri). *Vision Research, 32,* 833–842. [PubMed]

Packer, O., Hendrickson, A. E., & Curcio, C. A. (1990). Development redistribution of photoreceptors across the Macaca nemestrina (pigtail macaque) retina. *Journal of Comparative Neurology, 298,* 472–493. [PubMed]

Paquin, M. P., Hamam, H., & Simonet, P. (2002). Objective measurement of optical aberrations in myopic eyes. *Optometry and Vision Science, 79,* 285–291. [PubMed]

Porter, J., Guirao, A., Cox, I. G., & Williams, D. R. (2001). Monochromatic aberrations of the human eye in a large population. *Journal of the Optical Society of America A, Optics, Image Science, and Vision, 18,* 1793–1803. [PubMed]

Qiao-Grider, Y., Hung, L. F., Kee, C. S., Ramamirtham, R., & Smith, E. L., et al. (2007). Normal ocular development in young rhesus monkeys (Macaca mulatta). *Vision Research, 47,* 1424–1444. [PubMed] [Article]

Quick, M. W., & Boothe, R. G. (1992). A photographic technique for measuring horizontal and vertical eye alignment throughout the field of gaze. *Investigative Ophthalmology & Visual Science, 33,* 234–246. [PubMed] [Article]

Rabbetts, R. B. (1998). *Bennett & Rabbetts' clinical visual optics* (3rd ed.). Boston: Butterworth-Heinemann.

Ramamirtham, R., Kee, C. S., Hung, L. F., Qiao-Grider, Y., Huang, J., Roorda, A., et al. (2007). Wave aberrations in rhesus monkeys with vision-induced ametropias. *Vision Research, 47,* 2751–2766. [PubMed] [Article]

Ramamirtham, R., Kee, C. S., Hung, L. F., Qiao-Grider, Y., Roorda, A., & Smith, E. L., et al. (2006). Monochromatic ocular wave aberrations in young monkeys. *Vision Research, 46,* 3616–3633. [PubMed] [Article]

Riddell, P. M., Hainline, L., & Abramov, I. (1994). Calibration of the Hirschberg test in human infants. *Investigative Ophthalmology & Visual Science, 35,* 538–543. [PubMed] [Article]

Rucker, F. J., & Wallman, J. (2008). Cone signals for spectacle-lens compensation: Differential responses to short and long wavelengths. *Vision Research, 48,* 1980–1991. [PubMed]

Schaeffel, F., Glasser, A., & Howland, H. C. (1988). Accommodation, refractive error and eye growth in chickens. *Vision Research, 28,* 639–657. [PubMed]

Schaeffel, F., Hagel, G., Eikermann, J., & Collett, T. (1994). Lower-field myopia and astigmatism in amphibians and chickens. *Journal of the Optical Society of America A, Optics, Image Science, and Vision, 11,* 487–495. [PubMed]

Schaeffel, F., & Howland, H. C. (1988). Visual optics in normal and ametropic chickens. *Clinical Vision Sciences, 3,* 83–98.

Schmid, K., & Wildsoet, C. F. (1997). Natural and imposed astigmatism and their relation to emmetropization in the chick. *Experimental Eye Research, 64,* 837–847. [PubMed]

Schwiegerling, J. (2002). Scaling Zernike expansion coefficients to different pupil sizes. *Journal of the Optical Society of America A, Optics, Image Science, and Vision, 19,* 1937–1945. [PubMed]

Smith, W. J. (2000). *Modern optical engineering* (3rd ed.). Toronto, Canada: McGraw-Hill.

Spooner, J. D. (1959). *Ocular anatomy; the anatomy, histology, embryology, ontogeny, and phylogeny of the human eye and related structures.* London: Hatton Press.

Springer, A. D., & Hendrickson, A. E. (2005). Development of the primate area of high acuity, 3: Temporal relationships between pit formation, retinal elongation and cone packing. *Visual Neuroscience, 22,* 171–185. [PubMed]

Straznicky, C., & Chehade, M. (1987). The formation of the area centralis of the retinal ganglion cell layer in the chick. *Development, 100,* 411–420. [PubMed] [Article]

Tabernero, J., Benito, A., Alcon, E., & Artal, P. (2007). Mechanism of compensation of aberrations in the human eye. *Journal of the Optical Society of America A, Optics, Image Science, and Vision, 24,* 3274–3283. [PubMed]

Thibos, L. N., Cheng, X., Phillips, J., & Collins, A. (2002). Optical aberrations of chick eyes. *Investigative Opthalmology & Visual Science, 42,* 180.

Thibos, L. N., Hong, X., Bradley, A., & Applegate, R. A. (2004). Accuracy and precision of objective refraction from wavefront aberrations. *Journal of Vision, 4,* 329–351, http://journalofvision.org/4/4/9/, doi:10.1167/4.4.9. [PubMed] [Article]

Thibos, L. N., Hong, X., Bradley, A., & Cheng, X. (2002). Statistical variation of aberration structure and image quality in a normal population of healthy eyes. *Journal of the Optical Society of America A, Optics, Image Science, and Vision, 19,* 2329–2348. [PubMed]

Tian, Y., & Wildsoet, C. F. (2006). Diurnal fluctuations and developmental changes in ocular dimensions and optical aberrations in young chicks. *Investigative Ophthalmology & Visual Science, 47,* 4168–4178. [PubMed] [Article]

Wallman, J. (1991). Retinal factors in myopia and emmetropization: Clues from research on chicks. In T. Grosvenor & M. C. Flom (Eds.), *Refractive anomalies* (pp. 268–286). Boston: Butterworth-Heinemann.

Wallman, J., Turkel, J., & Trachtman, J. (1978). Extreme myopia produced by modest change in early visual experience. *Science, 201,* 1249–1251. [PubMed]

Wallman, J., & Winawer, J. (2004). Homeostasis of eye growth and the question of myopia. *Neuron, 43,* 447–468. [PubMed]

Wang, J., Candy, T. R., Teel, D. F., & Jacobs, R. J. (2008). Longitudinal chromatic aberration of the human infant eye. *Journal of the Optical Society of America A, Optics, Image Science, and Vision, 25,* 2263–2270. [PubMed] [Article]

Wang, J. Y., & Candy, T. R. (2005). Higher-order monochromatic aberrations of the human infant eye. *Journal of Vision, 5*(6):6, 543–555, http://journalofvision.org/5/6/6/, doi:10.1167/5.6.6. [PubMed] [Article]

Wetherell, W. B. (1980). The calculation of image quality. In R. R. Shannon & J. C. Wyant (Eds.), *Applied optics and optical engineering* (pp. 171–315). Toronto, Canada: Academic Press.

Williams, R. A., & Boothe, R. G. (1981). Development of optical-quality in the infant monkey (Macaca nemestrina) eye. *Investigative Ophthalmology & Visual Science, 21,* 728–736. [PubMed] [Article]

Wilson, B. J., Decker, K. E., & Roorda, A. (2002). Monochromatic aberrations provide an odd-error cue to focus direction. *Journal of the Optical Society of*

America A, Optics, Image Science, and Vision, 19, 833–839. [PubMed]

Yuodelis, C., & Hendrickson, A. (1986). A qualitative and quantitative analysis of the human fovea during development. *Vision Research, 26,* 847–855. [PubMed]

Zadnik, K., Mutti, D. O., Fusaro, R. E., & Adams, A. J. (1995). Longitudinal evidence of crystalline lens thinning in children. *Investigative Ophthalmology & Visual Science, 36,* 1581–1587. [PubMed] [Article]